ISSN: 0067-2904

Inhibitory Effects of Biosynthesized Copper Nanoparticles on Biofilm Formation of *Proteus mirabilis*

Noor Hamza Faiq*, Mais E.Ahmed
Department of Biology, College of Science, University of Baghdad, Baghdad, Iraq

Received: 23/10/2022 Accepted: 18/2/2023 Published: 30/1/2024

Abstract

This study aimed to explore whether green synthesized copper nanoparticles (CuNPs) can function as an anti-biofilm agent produced by *P. mirabilis*. The nanoparticles were synthesized from cells free extract of *P. mirabilis*. Characterization of biosynthesized copper nanoparticles was carried out to determine the chemical and physical properties of the product using atomic-force microscopy (AFM), transmission electron microscopy (TEM), field emission scanning electron microscopy (FESEM), X-ray diffraction (XRD) and UV-visible spectroscopy. The hexagonal structure was confirmed by XRD, size range was marked 13-19nm by TEM. FESEM was used to confirm the surface morphology. AFM analysis was used to reveal the roughness and distribution of nanoparticles. UV–visible spectra of the synthesized nanoparticles recorded a maximum peak at 380 nm. Copper nanoparticles showed remarkable biofilm inhibitory effects on wild type strains of multidrug resistant *Proteus mirabilis*.

After incubation for 24 and 48 hours at 37ºC with 128 µg/ml sub minimum inhibitory concentration (MIC) of CuO nanoparticles, strong biofilm producer strains showed weak biofilm production. Down regulation changes in *LuxS* expression using real time PCR technology were detected after treatment with copper nanoparticles of these strains.

Keywords: *Proteus mirabilis*, Biofilm, Copper nanoparticles, Antibacterial effect, Green synthesized nanoparticles.

التأثير المثبط لدقائق اوكسيد النحاس النانوية المصنعة حيوياً على تكوين الغشاء الحيوي لبكتيريا *Proteus mirabilis*

نور حمزة فائق، ميس عماد احمد
قسم علوم الحياة ، كلية العلوم، جامعة بغداد، بغداد، العراق

الخلاصة

هدفت هذه الدراسة الى التحري عن قدرة دقائق اوكسيد النحاس النانوية المصنعة حيوياً على تثبيط تكوين الغشاء الحيوي المنتج من قبل بكتيريا *Proteus mirabilis*. أُنتجت هذه الدقائق بأستعمال راشح بكتيري يحتوي على الانزيمات المختزلة لملح النحاس واستخدمت عدة تقنيات لتحديد الصفات الفيزيائية المظهرية لدقائق النانو المنتجة، فقد استخدمت تقنية XRD لتأكيد التركيب خماسي الشكل لهذه الدقائق، بينما أُستعملت تقنية TEM

*Email: nour.hamza1102a@sc.uobaghdad.edu.iq

لتحديد قطر الجزيئات المنتجة الذي تراوحبين 13 الى 19 نانومتر . اما تقنية FESEM فقد تم استخدامها لتحديد الصفات الخارجية لسطح جزيئات النانو المُنتجة، تم تأكيد النتائج بإستخدام تقنية AFM للكشف عن توزيع و خشونة جزيئات النانو.اما UV فقد سجلت اقصى امتصاصية عند الطول الموجي 380 نانومتر .تم التحري في هذه الدراسة عن فعالية دقائق اوكسيد النحاس النانوية في منع تكون الغشاء الحيوي حيث أُستعمل مستحلب دقائق اوكسيد النحاس النانوي بالتركيز تحت القاتل (128مكغ/مل). سجلت نتائج هذه الدراسة انخفاضا ملحوظًا في انتاج الغشاء الحيوي المنتج بكتيرياً، فقد سجلت العزلات ذات الانتاجية العالية للغشاء الحيوي ضعفاً في الانتاج بعد معاملتها بالتركيز المستعمل من دقائق اوكسيد النحاس النانوية. جاء تأثير هذه الدقائق على كل من النمط الظاهري والتعبير الجيني لجين *LuxS* المسؤول عن تكوين الغشاء الحيوي والذي تم الكشف عنهبإستخدام تقنية rtPCR، فقد سجلت الدراسة انخفاضا في التعبير الجيني لهذا الجين بعد معاملة سلالات البكتريا قيد الدراسة بدقائق اوكسيد النحاس النانوية.

Introduction

Several *Proteus* species are recognized as human causing disease pathogens, but only *Proteus mirabilis* is the one with the most frequent link to human disease. *P. mirabilis* is commonly associated with urinary tract infections (UTIs) in the individuals with structural or functional abnormalities. Patients undergoing urinary catheterization can also suffer from ascending infections [1]. Proteus has been shown to have the ability to produce biofilms in various situations from aquatic environments to indwelling devices, ureteral stents, scleral buckles, urethral catheters and tracheosophageal voice prostheses. *P. mirabilis* can also produce biofilms on biological as well as nonliving surfaces including glass, polystyrene, silicone, latex etc. [2].

Bacterial biofilms are well organized communities with single or multi species enclosed by a defensive polysaccharide matrix containing extracellular DNA, lipids and proteins [3]. The community of biofilm depends on complicated communications, enabling the pathogens to develop resistance against host defense mechanisms, different stress factors and antibiotics [4].
Bacterial biofilms are ubiquitous in clinical settings as they can increase bacterial resistance up to 1000 folds in compression to planktonic cells. Subsequently with anticipation measures taking place in hospitals and other clinical settings, nosocomial infections still result in major morbidity and mortality rate [5]. In this emergence situation, researchers are commended to improve new alternatives to traditional antibiotic treatments which can successfully combat against multidrug resistance (MDR) and biofilm producing bacteria.
Green synthesis of metal oxide NPs has gained a great interest since it is clean, eco-friendly approach and has a wide range of applications in biotechnology and medical field [6]. Copper nanoparticles (CuONPs) are of great interest due to their extraordinary properties such as flexibility high surface-to-volume ratio and rigidity.

Metal NP synthesis using microorganisms has represented a novel alternative to chemical and physical approaches as antibacterial, antioxidant and antifungal agents along with anticancer properties in various applications [7].

Several studies were interested in investigating the antibacterial activity of CuO. Noor *et al*. revealed a moderate antibacterial activity of fungal mediated CuO NPs against *E. coli, K. pneumoniae* and other gram-negative bacteria [8].

This study was aimed to determine the anti-biofilm activity of eco-friendly green synthesized copper oxide nanoparticles on biofilm production by *P. mirabilis.* Changes in *LuxS* expression was also investigated in this study.

Materials and Methods

Sample Collection:

A total of 100 urine samples were collected from patients that had urinary tract infection and resident hospital patients with urine catheters presented to Al Yarmouk teaching hospital.
Isolation and identification: *P. mirabilis* was primarily identified by culturing it on MacConkey and blood agar at 37°C for 24 h. and confirmed by VITEC 2 system.

Antibiotic Susceptibility Test:

According to CLSI 2021, susceptibility test took place using disk method on Mueller Hinton agar plates. The used antibiotics were levofloxacin 5 µg, ciprofloxacin 15 µg, ampicillin 25µg, gentamicin 10 µg, cefoxitin30 µg, ticarcillin + clavulanic acid 85µg, piperacillin-tazobactam 100/10 µg, cefepime µg, nitrofurnatoin 300 µg).

CuO Preparation

As a precursor, copper (II) and acetate Cu $(CH_3COO)_2 \cdot H_2O$) were used in this research.

Bacterial Suspension Preparation

P. mirabilis were grown in 250 ml of brain heart broth at 37°C for 24 hours in non-shaking incubator. The bacterial broth was then centrifuged, and the supernatant was collected after discarding the sediment.

Synthesis of CuO NPs

CuO NPs were synthesized by precipitation method. Later 20g of copper (II) acetate were added to 200ml of *P. mirabilis* cells free extract at room temperature 37^{o}C, sealed and covered with black plastic bag. After incubation in a shaker incubator for 24 h, the mixture then centrifuged, and the precipitate was collected and washed thrice by deionized water. Nanoparticles were synthesized by the extra cellular route where metal ions got reduced by the action of bacterial reducing enzymes. Nanoparticles formation can be detected by color change. The precipitant was later air dried and kept for further characterization [9]

Characterization of CuO NPs

Characterization is essential for understanding nanoparticles properties. The following methods were used to determine NPs characteristics. SEM and TEM were used to determine the shapes and sizes. SEM is used to characterize and visualize surface morphology, particle size distribution, particle/crystal shape, agglomeration of nanoparticles and surface functionalization and in single-particle analysis. TEM uses an electron beam to image a nanoparticle samples, providing much higher resolution than is possible with light-based imaging techniques. Atomic force microscopy (AFM) is used to define height and volume of NPs in 3D vision, UV–visible- (UV-DRS) is used to study the optical property of the samples. XRD is a technique that is used in materials science to determine the crystallographic structure of a material [10].

MIC Determination:

The estimation of minimum inhibitory concentration (MIC) was carried out to obtain the minimum concentration of CuO nanoparticles that inhibits bacterial growth by broth microdilution method using Eppendorf tubes. The bacterial inoculum was prepared in MHB and the concentration was modified to 100 UFC/µl. Two fold serial dilutions of CuO NPS were prepared in 16, 32, 64,128, 256, 512 µg/µl using MHB in six tubes which were then incubated

for 24 hours at 37°C. Results were later achieved by detecting visible growth of bacteria in each tube. Sub MIC can then be determined.

Estimation of Biofilm Formation

Quantitative determination of biofilm formation was perfomed by a colorimetric microtiter plate assay [11].

1- Brain heart infusion broth supplemented with an additional 1% glucose was used for this assay

2- Biofilm inoculums for cultivation were made from bacteria cultivated in broth, diluted 1:100 and poured into the well with 200 µl. Negative control wells was 200 µl of BHI supplemented with 1% glucose per well.

3- Under static conditions, the inoculated plate was covered with a lid and incubated aerobically for 24–30 hours at 35–37°C.

4- The contents of the wells were decanted, and each well was washed three times with 300 µl of PBS (2.2.5.1). The plates were then drained inverted and fixed with 150 ml methanol.

5- Staining was done with 150 µl of crystal violet at room temperature for 15 min, then washed and dried at room temperature.

6- For dye re-solubilizing, 150 µl of 95 percent ethanol was added, and the microtiter plate was covered with the lid and left at room temperature for at least 30 min., without shaking.

7- Using a microtiter-plate reader (GloMax/ Promega-USA), the optical density (OD) of each well was measured at 630 nm, and the results obtained are as following:

$OD \leq ODc$ = No biofilm producer,

$ODc < OD \leq 2\ ODc$= Weak biofilm producer,

$2\ ODc < OD \leq 4\ ODc$ = Moderate biofilm producer,

$4\ ODc < OD$= Strong biofilm producer.

The cut-off value for the negative control is ODc, which is defined as three standard deviations (SD), above the mean OD of the negative control: ODc= average OD of negative control + (3× SD of negative control).

Effects of CuO NPs on Biofilm Formation

This assay was carried out by 96- well microtiter plate as performed by Punniyakotti. *et al.* [12]. Tested isolates were cultured in brain heart infusion broth at 37^{o}C for 24h. Later 100 µl of bacterial inoculum was attuned to 0.5 McFarland and was then added to each well. Next 100 µl of CuO suspension was add to each well at the sub-inhibitory concentration before incubating the tubes at 37^{o}C for 48h. A positive control was presented as bacterial culture without nano formulations, while clear broth was considered as negative control. The contents of each well were discarded after incubation. Microplate was rinsed thrice with sterile saline and dried for 45 min at 60^{o}C. Next 200 mL of 0.1% of crystal violet was used in staining, followed by incubation at room temperature for 15 min. The microplate was rinsed three times with sterile normal saline and then acetic acid at 30% was added to each well by 200 ml. The optical density (OD) was read at 630 nm for all wells using a microtiter plate reader.

RT-qPCR Protocol

The presence of *LuxS* and *rpo* of *P. mirabilis* was determined by employing the thermal cycler to amplify the isolated genomic DNA (Thermo Fisher Scientific, USA). This main step can be separated into two stages: first stage is done by synthesis of cDNA from RNA using specific primer for *LuxS, rpo* transcripts (Table 1) and proto script cDNA synthesis kit. This procedure was performed as detailed in the manufacture procedure.

The second stage of this protocol was done by taking cDNA sample from tested isolates and control at the same run. For each sample, there were three PCR tubes, one tube for *LuxS* gene, *rpo* which is considered as a house keeping gene in this study. Fluorescent power of SYBR Green was used for quantity estimation. The reaction mix of component with their quantity is mentioned below in Table 2.

Table 1: Primers used in this study

Primer Name		Sequence	Product Size (bp)	Reference
***lux*S**	F	5'- TTCGCCAATGGGATGTCGTA-'3	474	[13]
	R	5'- TCCATAGCTGCCTTCCATGC-'3		
rsbA	F	F 5- CTATACCTACCGCACCATGT-3	467	[14]
	R	5- GAAGTCCCATCCGTTGATAC-3		
	R	5'- AGGCTGACGAACATCACGTA-'3		

Table 2: Synthesis of cDNA from RNA using primers for *LuxS*, *rpo* transcripts

Component	
Luna Universal Master Mix	10ul
Forward primer	1 ul
Reverse primer	1 ul
Template DNA	5 ul
Nuclease-free Water	3ul
Total volume	20ul

The difference in cycle thresholds (Ct) and fold changes between the treated groups and the calibrators for each gene were evaluated [15]. The *rpo* values were used to normalize the data. PCR tubes were spanned, and the liquid was collected (1 minute at 2000g)., Then the program for Real-Time PCR was setup with indicated thermos cycling protocol. The result was collected and analyzed by using Livak formula. Relative quantitation was applied to determine expression levels.

Statistical Analysis

All experiments were performed in triplicate and data was expressed as mean and standard deviation. The effect of study variables on biofilm was tested using the T test. The statistical analysis was done using Statistical Package For The Social Sciences (SPSS), version 26 software. The differences were considered significant when $p<0.05$.

Results and Discussion

Isolation and Identification:

Sixty-four isolates were confirmed as *P. mirabilis*. The confirmation was carried out by VITEK 2 system that is considered as a reliable identification technique, in addition swarming on blood agar and colony morphology on MacConkey agar.

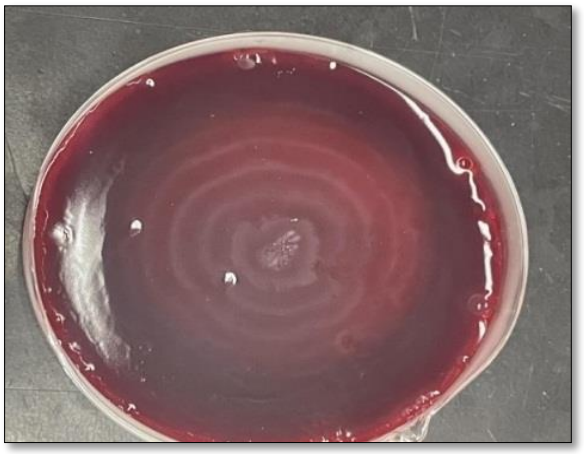

Figure 1: *Proteus mirabilis* on blood agar at 37ºC for 24h. incubation

Antibiotic Susceptibility Test

MDR Strains Screen:

After incubation at 37ºC for 24 hours, forty out of sixty-four isolates (62.5%) were confirmed as MDR strains. All tested isolates were resistance to piperacillin-tazobactam. Six isolates (15%) only were resistant to levofloxacin, while six isolates (15%) were found to be resistant to ciprofloxacin. Ampicillin did not inhibit growth of 15 isolates (37.5%) and gentamicin resistance was found in two strains only (5%). Six isolates (15%) were recorded as cefoxitin resistant and 17 isolates (42.5%) were resistant to nitrofurantoin.. A ten-year study in 2019 showed a growing concern about antibiotic resistance in proteae (Proteae tribe includes the genera Proteus, Morganella and Providencia). Based on the results of the study, resistance rates to third-generation cephalosporins developed significantly (the indicator during the study was ceftriaxone). Resistance to ceftriaxone increased by three times in hospitalized patients samples [16]. Another study carried out in China stated that 25 isolates of 54 *P. mirabilis* were classified as MDR. The samples were collected from wildlife animals and humans. This study highlighted that *P. mirabilis* produces AmpC β-lactamases and extended spectrum β-lactamases that makes this bacteria a serious public health risk. *P. mirabilis* also uses efflux pump to resist the main classes of antibiotics [17]. Resistance to cefotaxime also recently investigated by the detection of *blaCTX-M-1, blaCTX-M-2, blaCTX-M-8* and *blaCTX-M-9* that are responsible for cefotaxime resistance in *P. mirabilis* in the clinical isolates from urine samples in patients referred to different hospitals in Baghdad city [18].

Biosynthesis of Copper Oxide Nanoparticles:

Copper oxide nanoparticles were biosynthesized from *P. mirabilis*. The formation of nanoparticles was indicated by color change from yellow to blue, in addition to form a light blue precipitate. After centrifugation, the precipitate appeared greenish blue and after drying in the microwave, we obtained shiny blue powder, as shown in Figure 4. In recent years, an obvious coordination to use bacteria to synthesizes nanomaterials (mainly silver, zinc, gold, and nanoparticles) with remarkable properties have been observed for the development antimicrobials with *in vitro* activities against pathogenic bacteria [19]. Bacteria is an easy culturing microorganism with short generation time which makes bacteria a great candidate for nanoparticle synthesis as they have extra cellular reduction enzymes [20]. Several types of bacteria such as *E. coli, Pseudomonas fluoresces Serratia sp*., and *Pseudomonas stutzeri* have proved their ability to reduce certain metal ions and produce nanoparticles [21].

Figure 2: Biosynthesis of CuO Nano particles powder.

Characterization of CuO NPs

1- UV–Vis Spectral Analysis

The results showed that biosynthesized CuoNps exhibited a maximum peak at 380 nm. Smaller particle size was indicated previously at sharp peak observation at 270 nm as reported by Kayani *et al*. [22]. As shown in (Figure 3).

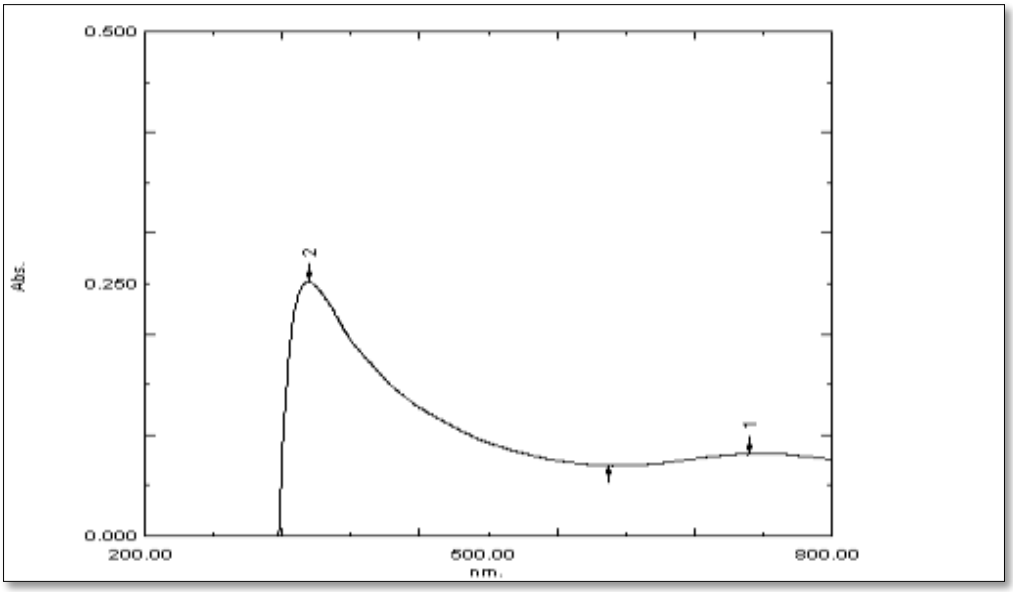

Figure 3: UV–Vis Spectrophotometry of Synergistic CuO Nps.

2- Atomic Force Microscopy (AFM) Analysis

AFM analysis of CuO NPs was performed to identify and characterize distribution of nanoparticles. Estimated grain size and mean square roughness were also determined. In Figure 6, portraits three-dimensional profile of CuONPs; 3D image of the CuO nanoparticles shows that the grains were distributed between 13 to 37nm [23].

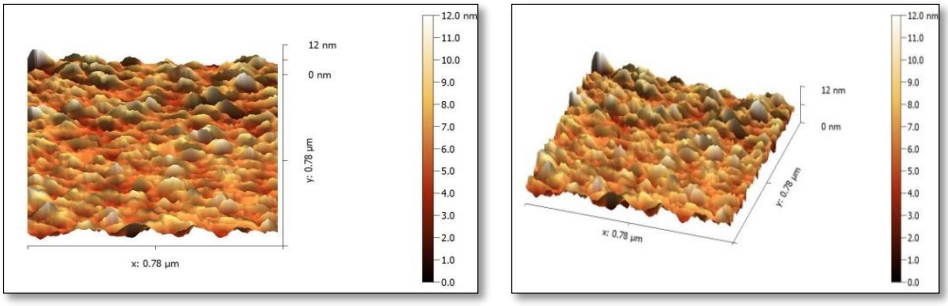

Figure 4: 3D AFM observation for CuO NPS.

3- Transmission Electron Microscopy Analysis (TEM)

TEM imaging was used to explore the morphology and size of CuO NPs. The core structure of the nanoparticles was confirmed by TEM analysis [20]. TEM images (Figure 5) demonstrate the formation of spherical shaped particles that were in 13-19nm range, with 77.5 kilo pixel magnifications and 40 nm resolution powers.

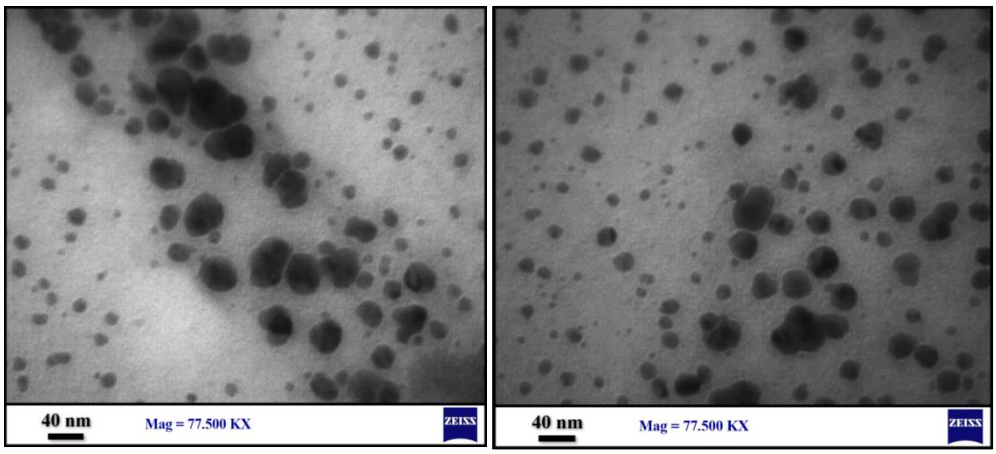

Figure 5: The TEM images of CuoNps show spherical shape of particles.

4- Field Emission Scanning Electron Microscope (FESEM)

SEM analysis was performed to understand the morphology and size, as well as the elemental and structural composition of NPs samples. Figure 8 shows the spherical shape of CuO NPs at 3000kv and 40000 magnification power. SEM images revealed that it was essentially spherical and uniform in appearance with the diameter ranging from 15 to 19nm. In comparison with EDX-ray, FESEM allows to determine the presence of different components in the examined model [20].

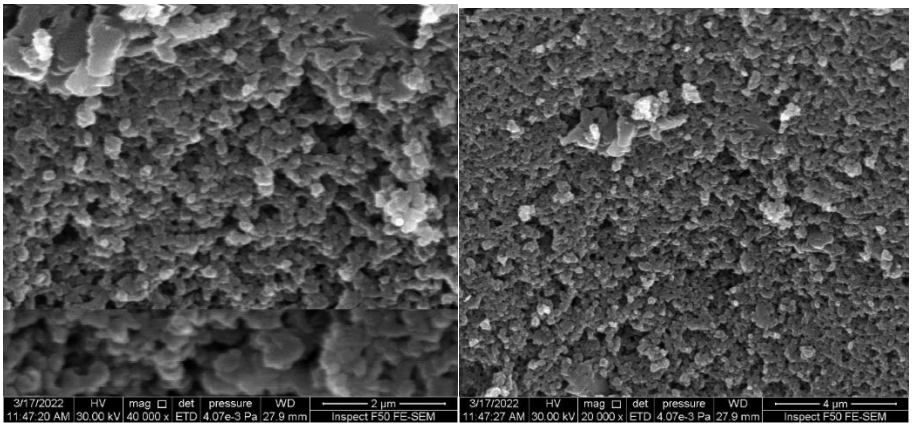

Figure 6: SEM Images of CuO NPs.

5-X-ray Diffraction (XRD)

The XRD spectra of CuO Nps powder shown in Figure 9, confirmed formation of hexagonal structure of the CuO NPs by revealing six prominent peaks corresponding to the diffraction peaks (16.414), (18.414), (22.278), (23.983), (26.113), and (43.537). One recent study has reported that the XRD pattern of the synthesized copper nanoparticles has the same peaks as those displayed by the XRD pattern of the same copper nanoparticles sample after being exposed to air for 24 h [24]. According to the International Center of Diffraction Data, the

crystalline points characterization was carried out by comparison with crystallographic standard data.

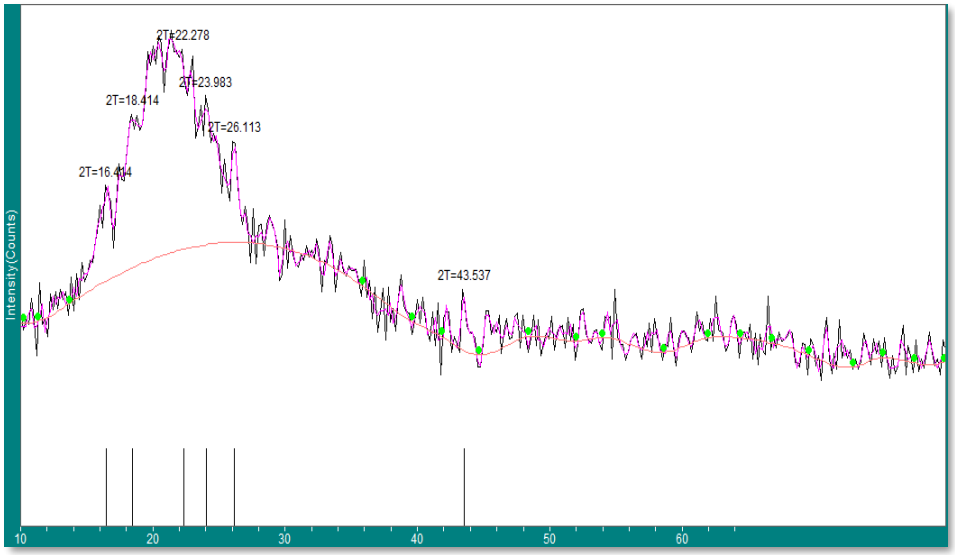

Figure 7: XRD analysis of green synthesized CuO NPs.

Determination of Biofilm Formation before CuO NPs Treatment

A total of 20 XRD isolates were tested for their biofilm production ability using a plastic microtiter plate. Of which nine isolates were recorded as strong biofilm producers as detailed in Table 2. To estimate the CuO NPs effects on biofilm production of these isolates, five strong producers strains were selected. OD of each well was read at 630 nm using a microtiter plate reader.

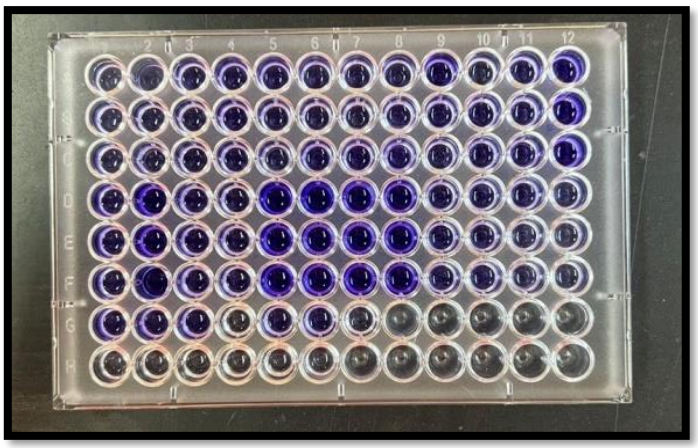

Figure 8: Microtiter plate assay for biofilm production.

Determination of Biofilm Formation after CuO NPs Treatment

Biofilm production was significantly reduced after 48 hours of incubation at 37°C with sub MIC of CuO NPs. OD measurement of the same five strains of *P. mirabilis* lowered from strong to weak production. The percentage inhibition of biofilm formation caused by CuO NPs according to the following equation: Percentage inhibition = 100 -[{ OD after treatment / OD before treatment x 100] as detailed in Table 3.

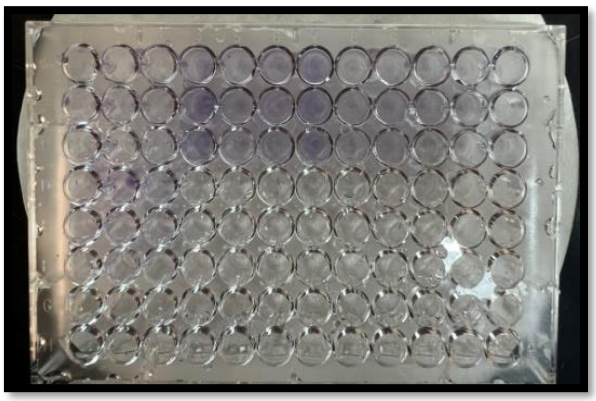

Figure 9: Biofilm production after treatment with CuO NPs Sub MIC.

Table 3: Percentage of inhibition after treatment with CuO NPs.

No. of Isolate	O.D before Treatment	Percentage of Inhibition
1.	5.75	82.2%
2.	9.19	84.2%
3.	6.30	82.3%
4.	7.25	84.2%
5.	7.15	83.6%

*Cut off value (ODc) = Mean OD of negative controls + 3 (Standard Deviation of control).

Antimicrobial action can be explained due to the small particle size of CuO NPs because smaller materials can enter bacterial cell membranes and cause cell damage. One research detailed that NPs seem to be more effective when they have smaller than 39 nm of diameter because they have a greater surface of interaction and in turn can reach the intra cellular space of bacteria straightforwardly [25]. Regarding CuO-NPs, Kouhkan *et al*.displayed that the small size of the NPs could increase the antibacterial effects of these particles due to large surface area that increases their concentration [16]. Nanoparticles can act on many levels and target bacterial components such as eDNA that plays a key role in bacterial adhesion, aggregation, biofilm formation and structure, biofilm integrity, in addition to intercellular communication or QS for transfer of genetic information [26]. Protein inhibition can result in a total destruction of biofilm and planktonic bacterial cells as they are involved in varied functions. Therefore, proteins are one of the important targets in recent antimicrobial therapies [27]. A recent study found that LPS from Gram-negative bacteria like *P. aeruginosa, Salmonella enterica* and *E. coli* bind Au nanoparticles , and the binding strength depends on the interaction of LPS with polyelectrolytes. A strong interaction between anionic LPS and cationic NPs was detected by the authors [28] suggesting that electrostatic interactions played a major role in LPS interaction with NPs.

-Gene Expression of *LuxS*

RT-PCR reveals a major down regulation in *LuxS* expression after the exposure to CuO NPs suspension compared to normal gene expression in bacterial broth with no NPs involved (Table 4). *LuxS* is a transcript of structural operon *luxCDABF* that is responsible for production of auto inducer 2 (AI-2) which predominantly participates in cell to cell signaling in bacteria. After *luxS* is produced, AI-2 casts signals that is used to sense inter species interaction and its own cell density in a multi microbial population that has essential role in the virulence factors regulation [29]. This result corresponds with the phenotypic changes in biofilm formation in

microtiter plate experiment carried out in this research (Figure 9). This finding also matched with other reports of Rajalakshmi and Sangeetha (2017) [30]. Antibiofilm activity of metal oxide nanoparticles have gained a great interest in last decades, since biofilm is an important virulence factor that enables the bacteria to resist antibiotics [31].

Table 4: Gene expression changes before and after treatment with CuO NPs.

	Ct before Treatment			Ct after Treatment				
Isolate No.	Ct rpo	Ct *LuxS*	ΔCt	Ct rpo	Ct *LuxS*	ΔCt	ΔΔCt	Fold Change
P.1A	16.68	17.36	0.68	18.02	17.45	-0.57	0.84	0.558
P.2B	13.77	11.75	-2.02	11.23	10.75	-0.48	1.54	0.34
P.3C	12.4	10.91	-1.49	14.31	13.25	-1.06	0.43	0.74
P.4D	11.03	11.67	0.64	14.63	14.86	0.23	0.41	1.32
P.5E	10.31	10.47	0.16	10.62	10.69	0.07	-0.09	1.06

Fold change in gene expression reveals that *LuxS* was down regulated in response to copper oxide NPs in three out of five isolates of *proteus mirabilis.* Whereas, the other two isolates were almost not affected. This could be due to the development of bacterial resistance mechanisms to nanoparticles. Recent studies have entailed several possible mechanisms used by bacteria to overcome nanoparticles effects, specially by over expression of genes responsible for the production of biofilm components such as exopolysaccharides and development of resistance after many culture steps [32] or up-regulation of efflux pump proteins and molecular interactions (electrostatic interactions) [33] . Copper generates toxic hydroxyl radicals (OH -) that damage cell membranes of Gram-negative and positive bacteria [34]. Positively charged metal nanoparticles can create a strong bond with membranes which can lead to increase their permeability and, therefore, disruption of cell walls. The most important factors determining the interaction with nanoparticles is biofilm maturity and thickness. As shown by Peulen and Wilkinson, EPS are denser in mature biofilms. Hence, the number of pores and the pore sizes are extensively reduced in mature biofilms, making them difficult for nanoparticles to penetrate. Accordingly, the antimicrobial activity of nanoparticles is higher in younger biofilms [35].

Anti-biofilm activity of metal oxide nanoparticles has gained a great interest in last decades, since biofilm is an important virulence factor that enables the bacteria to resist antibiotics [31]. Several studies have approved that these particles have bactericidal and bacteriostatic activity. Raheem in 2020 revealed that CuO can reduce biofilm formation in *Pseudomonas fluorescenson* by tube method [36]. Another study showed that CuO nanoparticles acted as powerful antimicrobial agent against *Proteus volgaris*, according to diameter of inhibition zone [37]. Another study was conducted to determine the antibacterial activity of green synthesized copper oxide nanoparticles (CuO NPs) using *Aloe vera* against *S. aureus, P. aeruginosa, E. coli, S.epidermidis, P. oryzihabitans, C. freundii, E. Cloacae, P. vulgaris.* The results were promising for potency of using copper nanoparticles in toothpastes in concentration dependent manner [38].

Conclusion

An alarming situation has risen by multi-resistant bacterial strains that has driven the research in the direction of finding novel therapies to combat the infections and diseases associated with bacterial biofilms.

CuO NPs were successfully synthesized following an indirect, eco- friendly, low cost, high-yield and green method. CuO NPs showed exceptional antimicrobial activity against several bacterial strains. Thus, CuO NPs can be used for external usages as antibacterial agents by

coatings surfaces on various substrates to prevent biofilm producing microorganisms from attaching and colonizing in indwelling medical devices. In order to modulate the nature of nanoparticle–biofilm interactions is to make copper oxide nanoparticles highly selective against one component of the biofilm via bioconjugation techniques. Copper oxide NPs draped with different chemical moieties has proven to be fairly better than uncoated nanoparticles in terms of their interactions with the biofilm and antibacterial activity. Due to their effectiveness in all fields of science, nanoparticles application is increasing nowadays. green synthesized nano materials that are mostly used in drug delivery and medical approaches have some downsides in using these metal oxides because of their higher toxicity when used in higher concentration. All former conclusions highlight that there is an actual need for more investigation in order to use CuO-NPs as encouraging alternate antibacterial materials.

References

[1] M. H. Muhammad *et al.*, "Beyond risk: Bacterial biofilms and their regulating approaches," *Front. Microbiol.*, vol. 11, p. 928, 2020.

[2] M. Shokouhfard, R.-K. Kermanshahi, M.-M. Feizabadi, S. Teimourian, and F. Safari, "Lactobacillus spp. derived biosurfactants effect on expression of genes involved in Proteus mirabilis biofilm formation," *Infect. Genet. Evol.*, vol. 100, no. 105264, p. 105264, 2022.

[3] V. A. Spirescu *et al.*, "Biofilm-resistant nano-coatings based on ZnO nanoparticles and linalool," *Nanomaterials (Basel)*, vol. 11, no. 10, p. 2564, 2021.

[4] P. C. Balaure and A. M. Grumezescu, "Recent advances in surface nanoengineering for biofilm prevention and control. Part II: Active, combined active and passive, and smart bacteria-responsive antibiofilm nano-coatings," *Nanomaterials (Basel)*, vol. 10, no. 8, p. 1527, 2020.

[5] M. Kazemzadeh-Narbat *et al.*, "Strategies for antimicrobial peptide coatings on medical devices: a review and regulatory science perspective," *Crit. Rev. Biotechnol.*, vol. 41, no. 1, pp. 94–120, 2021.

[6] L. Sarcina *et al.*, "Cu nanoparticle-loaded nanovesicles with antibiofilm properties. Part I: Synthesis of new hybrid nanostructures," *Nanomaterials (Basel)*, vol. 10, no. 8, p. 1542, 2020.

[7] A. T. Khalil *et al.*, "Microbes-mediated synthesis strategies of metal nanoparticles and their potential role in cancer therapeutics," *Semin. Cancer Biol.*, vol. 86, no. Pt 3, pp. 693–705, 2022.

[8] S. Noor *et al.*, "A fungal based synthesis method for copper nanoparticles with the determination of anticancer, antidiabetic and antibacterial activities," *J. Microbiol. Methods*, vol. 174, no. 105966, p. 105966, 2020.

[9] M. A. Ali *et al.*, "Advancements in plant and microbe-based synthesis of metallic nanoparticles and their antimicrobial activity against plant pathogens," *Nanomaterials (Basel)*, vol. 10, no. 6, p. 1146, 2020.

[10] Y.-K. Phang *et al.*, "Green synthesis and characterization of CuO nanoparticles derived from papaya peel extract for the photocatalytic degradation of palm oil mill effluent (POME)," *Sustainability*, vol. 13, no. 2, p. 796, 2021.

[11] N. Jaffar, T. Miyazaki, and T. Maeda, "Biofilm formation of periodontal pathogens on hydroxyapatite surfaces: Implications for periodontium damage: Biofilm Formation of Periodontal Pathogens on Hydroxyapatite Surfaces," *J. Biomed. Mater. Res. A*, vol. 104, no. 11, pp. 2873–2880, 2016.

[12] R. Wasfi, G. R. Abdellatif, H. M. Elshishtawy, and H. M. Ashour, "First-time characterization of viable but non-culturable Proteus mirabilis: Induction and resuscitation," *J. Cell. Mol. Med.*, vol. 24, no. 5, pp. 2791–2801, 2020.

[13] K. J. K. K. A. M. S. S. A. Abbas, "Molecular detection of some virulence genes in Proteus mirabilis isolated from Hilla province," *Int. J. Res. Stud. in Biosci. (IJRSB)*, vol. 3, pp. 85–89, 2015.

[14] M. Gajdács and E. Urbán, "Comparative epidemiology and resistance trends of Proteae in urinary tract infections of inpatients and outpatients: A 10-year retrospective study," *Antibiotics (Basel)*, vol. 8, no. 3, p. 91, 2019.

[15] K. J. Livak and T. D. Schmittgen, "Analysis of relative gene expression data using real-time quantitative PCR and the 2-ΔΔct Method,"Methods," *Methods," methods*, vol. 25, pp. 402–408, 2001.

[16] M. Kouhkan, P. Ahangar, L. A. Babaganjeh, and M. Allahyari-Devin, "Biosynthesis of Copper Oxide Nanoparticles Using Lactobacillus casei Subsp. Casei and its Anticancer and Antibacterial Activities," *Curr. Nanosci.*, vol. 16, no. 1, pp. 101–111, 2020.

[17] Q. Kang *et al.*, "Multidrug-resistant Proteus mirabilis isolates carrying blaOXA-1 and blaNDM-1 from wildlife in China: increasing public health risk," *Integr. Zool.*, vol. 16, no. 6, pp. 798–809, 2021.

[18] D. N. F. Passat, "Local Study of blaCTX-M genes detection in Proteus spp. by using PCR technique"," *Iraqi Journal of Science*, vol. 57, no. 2C, pp. 1371–1376, 2022.

[19] G. Grasso, D. Zane, and R. Dragone, "Microbial nanotechnology: Challenges and prospects for green biocatalytic synthesis of nanoscale materials for sensoristic and biomedical applications," *Nanomaterials (Basel)*, vol. 10, no. 1, p. 11, 2019.

[20] J. Singh, T. Dutta, K. H. Kim, M. Rawat, P. Samddar, and P. Kumar, "'Green synthesis of metals and their oxide nanoparticles: applications for environmental remediation," *Journal of nanobiotechnology*, vol. 16, no. 1, pp. 1–24, 2018.

[21] P. Punniyakotti, P. Panneerselvam, D. Perumal, R. Aruliah, and S. Angaiah, "Anti-bacterial and anti-biofilm properties of green synthesized copper nanoparticles from Cardiospermum halicacabum leaf extract," *Bioprocess Biosyst. Eng.*, vol. 43, no. 9, pp. 1649–1657, 2020.

[22] F. Erci, R. Cakir-Koc, M. Yontem, and E. Torlak, "Synthesis of biologically active copper oxide nanoparticles as promising novel antibacterial-antibiofilm agents," *Prep. Biochem. Biotechnol.*, vol. 50, no. 6, pp. 538–548, 2020.

[23] B. Turakhia, M. B. Divakara, M. S. Santosh, and S. Shah, "Green synthesis of copper oxide nanoparticles: a promising approach in the development of antibacterial textiles," *J Coat Technol Res*, vol. 17, no. 2, pp. 531–540, 2020.

[24] E. Hoseinzadeh *et al.*, "A review on nano-antimicrobials: Metal nanoparticles, methods and mechanisms," *Curr. Drug Metab.*, vol. 18, no. 2, pp. 120–128, 2017.

[25] S. J. Kassinger and M. L. van Hoek, "Biofilm architecture: An emerging synthetic biology target," *Synth. Syst. Biotechnol.*, vol. 5, no. 1, pp. 1–10, 2020.

[26] E. A. Mohamed, "Green synthesis of copper & copper oxide nanoparticles using the extract of seedless dates," *Heliyon*, vol. 6, no. 1, p. e03123, 2020.

[27] N. S. Abadeer, G. Fülöp, S. Chen, M. Käll, and C. J. Murphy, "Interactions of bacterial lipopolysaccharides with gold nanorod surfaces investigated by refractometric sensing," *ACS Appl. Mater. Interfaces*, vol. 7, no. 44, pp. 24915–24925, 2015.

[28] E. I. Hussein *et al.*, "Assessment of pathogenic potential, virulent genes profile, and antibiotic susceptibility of Proteus mirabilis from urinary tract infection," *Int. J. Microbiol.*, vol. 2020, p. 1231807, 2020.

[29] R. Rajalakshmi, D. Sangeetha, and V. Udhaya, "Effect of Antifungal Drugs against Candida Isolates from Diabetic Women with Vaginitis," *Journal of Infectious Diseases and Therapy*, vol. 5, no. 4, pp. 2–5, 2019.

[30] S. Shah *et al.*, "Biofilm inhibition and anti-quorum sensing activity of phyto-synthesized silver nanoparticles against the nosocomial pathogen Pseudomonas aeruginosa," *Biofouling*, vol. 35, no. 1, pp. 34–49, 2019.

[31] N. Niño-Martínez, M. F. Salas Orozco, G.-A. Martínez-Castañón, F. Torres Méndez, and F. Ruiz, "Molecular mechanisms of bacterial resistance to metal and metal oxide nanoparticles," *Int. J. Mol. Sci.*, vol. 20, no. 11, p. 2808, 2019.

[32] A. S. P. A. M. I. Joshi, "interactions of gold and silver nanoparticles with bacterial biofilms: Molecular interactions behind inhibition and resistance," i*nternational Journal of Molecular Sciences,* vol. 21, no. 20, 2020.

[33] N. J. Mishu, S. M. Shamsuzzaman, H. M. Khaleduzzaman, and M. A. Nabonee, "Association between Biofilm Formation and Virulence Genes Expression and Antibiotic Resistance Pattern in Proteus mirabilis, Isolated from Patients of Dhaka Medical College Hospital," *Archives of Clinical and Biomedical Research*, vol. 6, no. 3, pp. 418–434, 2022.

[34] D. Sistemática, S. S. Gabriela, F. R. Daniela, and B. T. Helia, "Copper nanoparticles as potential antimicrobial agent in disinfecting root canals," *Odontostomat*, vol. 10, no. 3, pp. 547–554, 2016.

[35] T.-O. Peulen and K. J. Wilkinson, "Diffusion of nanoparticles in a biofilm," *Environ. Sci. Technol.*, vol. 45, no. 8, pp. 3367–3373, 2011.

[36] H. Raheem and H. Yasser, "Silver Nanoparticles as Antibacterial Action against Pseudomonas Fluorescens Isolated from Burn Infection," *Annals of the Romanian Society for Cell Biology}*, pp. 12578–12583, 2021.

[37] M. Ahamed, H. A. Alhadlaq, M. A. M. Khan, P. Karuppiah, and N. A. Al-Dhabi, "Synthesis, characterization, and antimicrobial activity of copper oxide nanoparticles," *J. Nanomater.*, vol. 2014, pp. 1–4, 2014.

[38] S. M. Abed, Y. S. Mahmood, I. F. Waheed, and A. M. Alwan, "Antibacterial Activity of Green Synthesized Copper Oxide Nanoparticles"," *Iraqi Journal of Science*, vol. 62, no. 9, pp. 3372–3383, 2021.